Nuclear Instruments and Methods in Physics Research B 106 (1995) 386–392

NIM B
Beam Interactions with Materials & Atoms

ELSEVIER

Materials issues and device performances for light emitting Er-implanted Si

S. Coffa [a,*], F. Priolo [b], G. Franzó [b], A. Polman [c], S. Libertino [b], M. Saggio [a], A. Carnera [d]

[a] *CNR-IMETEM, Stradale Primosole 50, I-95121 Catania, Italy*
[b] *Dipartimento di Fisica, Università di Catania, Corso Italia 57, I-95129 Catania, Italy*
[c] *FOM-Institute AMOLF, Kruislaan 407, 1098 SJ Amsterdam, The Netherlands*
[d] *Dipartimento di Fisica, Università di Padova, Via F. Marzolo 9, I-35131 Padova, Italy*

Abstract

The mechanisms of photo and electroluminescence from Er-implanted crystalline Si have been investigated and the crucial issues for the achievement of higher efficiency have been identified. Photoluminescence experiments show that Er-related levels are the gateway for the energy transfer from the electronic system of the semiconductor to the internal 4f shell of the Er ions. Er excitation is in fact thought to occur by the recombination of an electron–hole pair bound to an Er-related level. Higher yield and reduced temperature quenching of the luminescence can be obtained by engineering of the properties of these levels by codoping with O or other impurities. Room temperature electroluminescence has been achieved from Er doped crystalline Si diodes under both forward and reverse bias. Under forward bias the same mechanism identified from photoluminescence experiments is operative and therefore similar requirements have to be met in order to improve efficiency. On the other hand a higher room temperature electroluminescence yield is obtained under reverse bias. In this case the energy transfer occurs by impact excitation of the Er ions by hot carriers. Crucial issues for excitation mechanisms are the proper design of the diode structure in order to optimize the hot carrier distribution and the increase of the fraction of incorporated ions which are efficiently excited.

1. Introduction

The incorporation of rare-earth ions in semiconductors has been recognized [1–3] as a suitable method to combine the optical properties of these ions with the electronic properties of the semiconductor host. In particular it has been shown [1–7] that the sharp-atomic like emission, resulting from an internal 4f transition of these ions in their 3+ state, can be achieved when this shell is excited by an energy transfer through the electronic system of the semiconductor. For example excitation through electron–hole (e–h) recombination and through hot-carrier impact excitation have been demonstrated for Yb in InP [4] and for Er in GaAs [5]. Silicon is the leading semiconductor in the electronic industry and would be the material of choice when a combination of electronic and optical properties on the same chip is required. Nevertheless the indirect band gap and the lack of linear electro-optic effects make Si unsuitable particularly for optical functions such as light emission and light modulation. Rare-earth incorporation in Si could provide a method to circumvent the inability of Si to operate as a light source. Recently Er incorporation in Si has received noticeable interest [6–12] since the internal 4f transition of this ion occurs at 1.54 μm, a wavelength of large interest in telecommunications since it falls in a window of maximum transmission for the optical fibers. The possibility to excite Er through a carrier mediated process has been demonstrated and both photo- [6,9] and electroluminescence [11–13] at room temperature (RT) have been reported. Several investigations [9,14,15] have demonstrated that codoping with impurities, in particular O, enhances the photoluminescence yield of Er and reduces its temperature quenching. Therefore, understanding the role of O is crucial for the optimization of the light source and for the achievement of intense room temperature light emission needed for optoelectronic applications. This achievement also requires the understanding of the excitation mechanisms and the role that the electronic properties of the Er ions play in these mechanisms. In this work photo- and electroluminescence investigations of Er in crystalline Si (c-Si) are presented with emphasis on the current understanding

* Corresponding author. Tel. +39 95 59 1912, fax +39 95 7139154.

SSDI 0168-583X(95)00737-7

of the excitation processes, the role of oxygen codoping and the identification of the major limitations for the achievement of higher efficiency.

2. Excitation mechanisms

Due to the highly localized character of the 4f shell of the Er ion, a major problem for Er excitation is the energy transfer from the electronic system of the semiconductor to the Er ions. Theoretical investigations [16,17] have shown that the probability of Er excitation through the recombination of free carriers is quite low and only a very inefficient pumping can be obtained through this mechanism. On the other hand there are two mechanisms which are expected to be much more efficient:

(1) a recombination of an electron–hole pair with at least one of the carriers being localized at an Er-related deep level in the band gap. (The excitation process will occur either by an Auger process or by the recombination of an electron–hole pair bound to the level)

(2) impact excitation of the Er ions by hot carriers: the excitation occurs through the Coulomb interaction between the hot carriers and the electronic ground state of the 4f shell. This process is not mediated by a level in the band gap but, for energy conservation, it requires carriers with kinetic energy higher than 0.8 eV (the energy separation between ground and first excited state in the 4f shell). This mechanism therefore requires the achievement of nonequilibrium conditions in carrier distributions.

The first mechanism is the one operative under standard photoluminescence experiments when an Argon laser produces electron–hole pairs, the recombination of which produces Er excitation and light emission at 1.54 μm. The second mechanism might be operative, for example, in the depletion region of a reverse biased junction. We will first consider Er excitation in photoluminescence experiments.

2.1. Photoluminescence: the role of oxygen

In a photoluminescence experiment Er excitation occurs through the recombination of an e–h pair. This process is mediated by an Er-related level that guarantees the necessary coupling between the electronic system of Si and the internal 4f shell of Er ions. Moreover, the alternative recombination routes for e–h pairs, not ending up with Er excitation, should be suppressed. The efficiency of Er excitation is known to be enhanced by the presence of impurities such as O and F. At 77 K an increase in the PL yield can be obtained by codoping with those impurities. We have recently demonstrated [9,18] that impurities have also a large effect on the temperature quenching of the luminescence. The effect of O on temperature quenching is reported in Fig. 1. In this figure the PL intensity of 1.54 μm for Er in Si containing different oxygen concentrations is reported as a function of the reciprocal temperature. The data are taken at a pump power of 200 mW of the Ar ion laser and are normalized, for clarity, to the PL intensity at 77 K. The total amount of Er is in all cases $\sim 10^{15}$ Er/cm^2. The O content was varied by implanting Er in float zone (FZ) Si ($\sim 10^{16}$ O/cm^3), in Czochralski (CZ) silicon ($\sim 10^{18}$ / cm^3) or by coimplanting O in order to reach a uniform O concentration of 3×10^{19} or 1×10^{20} /cm^3. The data show that oxygen produces a large reduction in the temperature quenching. The PL intensity decreases far more rapidly in FZ-Si than CZ-Si as the temperature increases and quenching is further decreased at higher O concentration. In fact, while in CZ-Si the PL yield decreases by a factor of ~ 500 on going from 77 to 300 K, in Si doped with 10^{20} O/cm^3 this quenching, in the same temperature range is only a factor of ~ 30. In all cases, independently of the oxygen concentration, the PL temperature dependence is characterized by two well defined regimes. At low temperatures the PL decreases with a small activation energy while at higher temperatures the slope changes and the PL decreases with a small activation energy of ~ 0.15 eV. Oxygen produces a shift towards higher values of the temperature at which the 0.15 eV activated regime begins. These results can be understood in terms of the major changes that the Er–O interaction produces in the local environment around the Er atoms. In particular EXAFS analyses [14] have shown that Er is coordinated with 12 Si atoms in FZ silicon (low oxygen content) and with 6 O atoms in CZ silicon (high oxygen content). The interaction with oxygen also modifies the bonding character of Er in Si and hence the concentration and energy location of Er-related deep levels. In order to investigate these modifications we have performed deep level transient spectroscopy (DLTS) measurements on samples prepared as follows. Er was implanted at 5 MeV to a fluence of 6×10^{11} ions/cm^2 in epitaxial Si (with low impurity content). After implantation an annealing treatment was performed at 900°C for 30 s under nitrogen flux. The DLTS spectrum of this sample is reported in Fig. 2 (solid line) and reveals the presence of four well separated peaks on a continuous background. These peaks are localized at $E_c - 0.51$ eV (E_1), $E_c - 0.34$ eV (E_2), $E_c - 0.26$ eV (E_3), $E_c - 0.2$ eV (E_4), respectively (E_c indicates the bottom of the conduction band). The influence of oxygen on the electronic properties of Er in c-Si has been explored by coimplanting Er and O in the pure epitaxial Si. Er was implanted in the same condition (5 MeV, 6×10^{11} ions/cm^2) while multiple O implants at different energies were performed in order to realize a uniform O concentration at 10^{17}/cm^3 or 10^{18}/cm^3 in the region

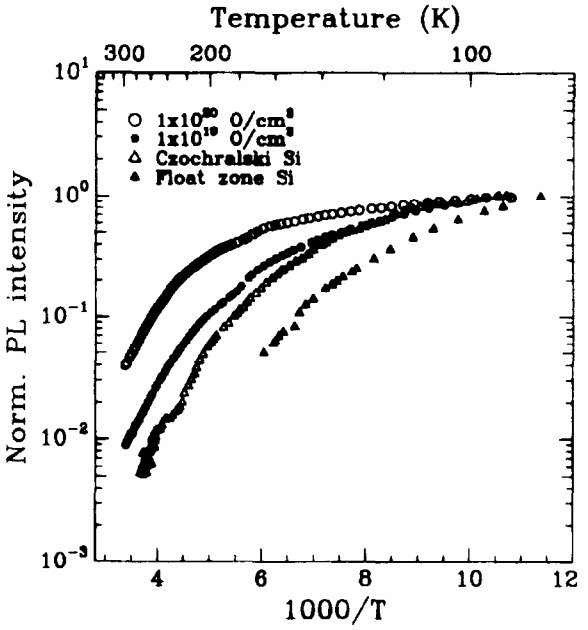

Fig. 1. Photoluminescence intensity at 1.54 μm versus the reciprocal temperature for Er in Si containing different O contents. The Er dose is in all cases $\sim 10^{15}$ /cm^2. The data are normalized to the photoluminescence intensity at 77 K.

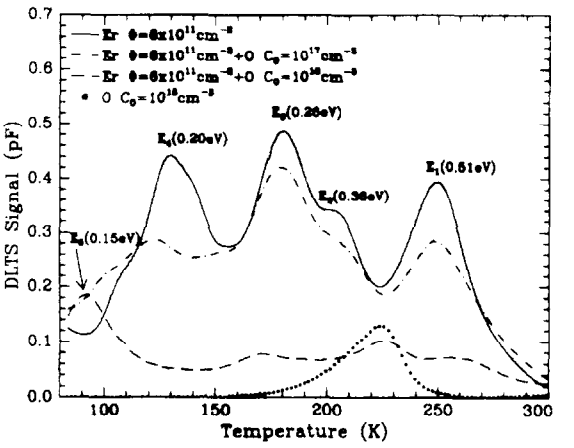

Fig. 2. DLTS spectra for solely Er implanted expitaxial silicon (solid line) and for samples coimplanted with O (multiple implants to achieve a uniform concentration of 10^{17} or 10^{18} O/cm^3). In each sample Er was implanted at 5 MeV to a fluence of 6×10^{11} /cm^2 and annealing was performed at 900°C for 30 s. The spectrum for a solely O implanted sample is also reported.

where Er sits. Annealing was again performed at 900°C for 30 s under nitrogen flux. As shown in Fig. 2, O produces major modifications in the deep level spectra. For the lowest oxygen concentration (10^{17}/cm^3) the intensities of the deepest levels are slightly reduced while a large change occurs in the structure of the shallower level E_4. In particular this level shifts to lower temperatures where a more complex structure starts to develop. These features are more strikingly evident for the highest O concentration (10^{18}/cm^3). In this sample the concentrations of deepest levels are reduced by about one order of magnitude and a new well defined peak at $E_c - 0.15$ eV (E_5) develops. This peak dominates the spectrum of this sample. It should be noted that this peak does not arise from the O implants only. In fact the spectrum of a sample solely implanted with oxygen is also reported in Fig. 2 and only reveals a peak $E_c - 0.34$ eV. Therefore the peak E_5 results from the interaction between Er and O. More extensive investigations [19] and the analysis of the annealing behaviour of these peaks allowed us to associate the levels E_1 through E_4 (characteristic of Er in pure c-Si) to Er-defect complexes and the level E_5 (characteristic of Er + O implanted samples) to an Er–O complex.

These results suggest that the role of O is at least twofold and are consistent with the following scenario. Er excitation occurs through the recombination between an electron bound to an Er-related level and a hole. The formation of Er–O complexes results in the introduction of a level at $E_c - 0.15$ through which efficient pumping can be achieved. The regime with an activation energy of 0.15 eV in the temperature quenching of the photoluminescence (Fig. 1) is caused by the thermalization of the electron, localized on the Er level, to the conduction band. This thermalization effectively inhibits energy transfer to the Er ions and causes the reduction of the PL yield at higher temperatures. The reduction in the concentration of the deepest levels, also produced by oxygen codoping (Fig. 2), causes a reduction in the magnitude of competitive recombination routes for the e–h pairs and produces both an enhancement of the pumping efficiency and a reduction of temperature quenching.

2.2. Electroluminescence: light emitting and electroluminescent diodes

We have also achieved room temperature electroluminescence by incorporating Er and O in a suitable diode structure. The diode consists of p^+–n^+ junctions realized as follows. We used a 5 μm thick n^- doped epitaxial layer grown on a n^+ substrate. Through a photolithographically defined window Er + O implants are performed followed by a shallow B implant. Erbium and oxygen were introduced by multiple implants in order to realize a 2 μm thick region with 10^{19} Er/cm^3 and 10^{20} O/cm^3. After regrowth at 620°C for 3 h and further annealing at 900°C for 30 s, electrical measurements showed that a junction is formed at a depth of 0.35 μm as a result of the B profile (p^+ side) and the Er + O profile (n^+ side, due to the well known enhancement of the donor behaviour of Er in the

presence of O). Back and front side metallization completed the device structure. The front side metallization has a stripe geometry with an open area of 50% in order to allow the light to exit. From these diodes we have obtained light emission under both forward and reverse bias. Fig. 3a shows the electroluminescence spectrum obtained at room temperature under forward bias at a current density of 2.5 A/cm^2. The well defined structured spectrum of Er is observed on a flat background. Under reverse bias at breakdown ($\sim$ 5 V), still at room temperature, and with the same current density passing through the device, a much higher signal is observed. This signal is about 16 times higher than its forward bias counterpart as shown in Fig. 3b. This well defined and intense Er peak sits on a very broad background which is essentially flat in the wavelength region where the germanium detector we used is sensitive (0.8–1.7 μm). Such a background was not observed in forward bias. This broad emission is known to occur in reverse biased junctions [20] and has been attributed to hot carrier transition either as a consequence of bremsstrahlung or of intraband transitions [21]. As a matter of fact this spectrum is not confined to the infrared region but it also extends to the visible

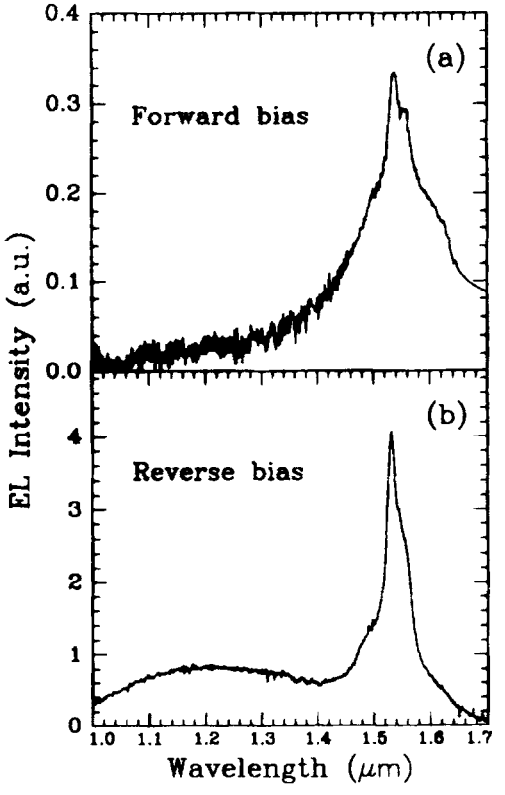

Fig. 3. Room temperature electroluminescence spectra from Er + O implanted Si diodes under forward (a) and reverse (b) bias. The spectra are taken at a current density of 2.5 A/cm^2.

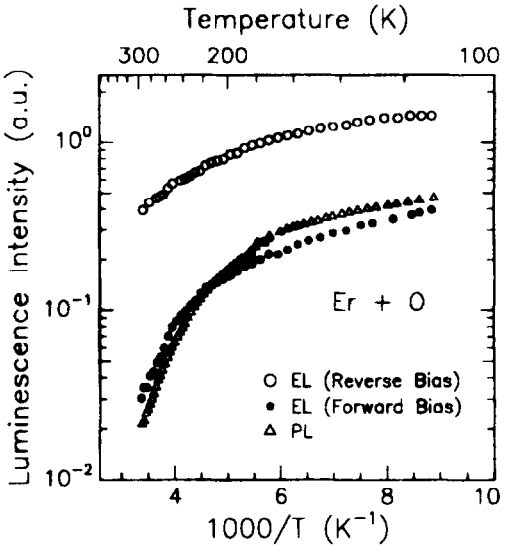

Fig. 4. Electroluminescence intensity at 1.54 μm versus the reciprocal temperature under reverse (O) and forward bias (●). All the measurements have been made for a constant current density of 2.5 A/cm^2 through the device. For comparison the temperature dependence of the PL yield is also shown (△). For clarity of comparison this last curve was divided by a factor of 6.

as a red glow is detectable in the dark by the naked eye. Electroluminescence under reverse bias also exhibits a different temperature dependence when compared to its forward bias counterpart. In fact, as reported in Fig. 4, a decrease by only a factor of 4 is observed between 77 K and RT. In contrast, the EL intensity under forward bias decreases by a factor of 30 in the same temperature range in a similar fashion as the PL intensity measured on similar samples and also reported in Fig. 4. These results suggest that the same excitation mechanism is operative in photoluminescence and forward bias electroluminescence. On the other hand the larger efficiency of EL under reverse bias and its different temperature dependence suggest that a different mechanism might be operative. The clear evidence presented by the presence of hot carriers in the reverse biased diode strongly supports the idea that Er excitation is now occurring through impact excitation.

In order to understand how hot carriers are created in the structure it is necessary to investigate the breakdown mechanisms of these diodes in detail. In Fig. 5 measurements of the reverse I–V characteristics for different temperatures are reported. Breakdown of these diodes occurs already at low voltages ($\sim$ 5 V at RT) and the critical voltage decreases by increasing temperature. Solid lines in Fig. 5 are simulations of the I–V characteristics of the adopted diode structure us-

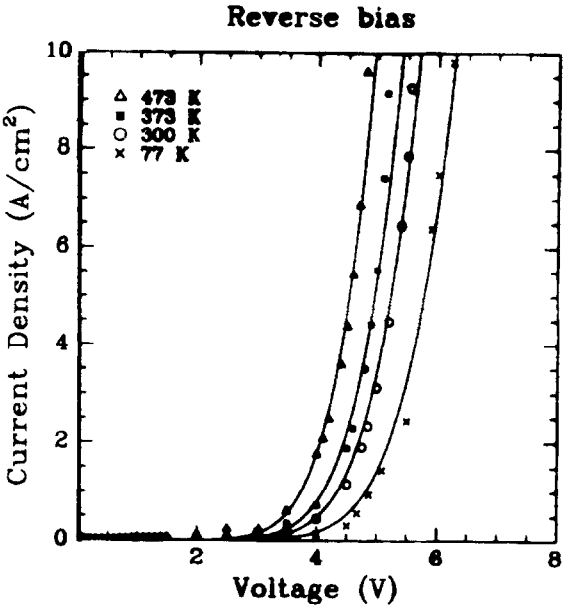

Fig. 5. Current density versus voltage for the diodes in reverse bias at different temperatures. The lines are fits obtained using a device simulator (see text).

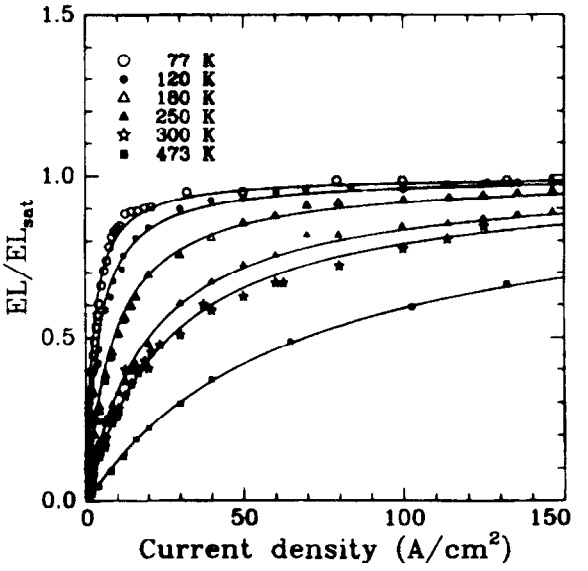

Fig. 6. Electroluminescence yield as a function of current density at different temperature. The yield (EL) is normalized to the saturation value (EL_{sat}) obtained at high current density. At all temperatures the same EL_{sat} value is used to normalize the data.

ing PISCES [22], a device simulator, and assuming that the breakdown occurs by band to band tunneling. The experimental results and the simulations clearly indicate that breakdown occurs by band to band tunneling (Zener mechanism) through which a valence band electron is promoted to the conduction band. This electron (and the corresponding hole left in the valance band) are generated in the depletion region of the junction where an electric field is present. They are therefore accelerated and can become hot enough to impact ionize the Er ions. Assuming that the emitted electrons only collide with optical phonons it is possible to derive [23] that their distribution is Maxwellian and calculate the characteristic temperature which corresponds to ~ 0.65 eV. For this temperature $\sim 40\%$ of the electrons of the distribution will have enough kinetic energy to ionize Er (larger than 0.8 eV). As shown in Fig. 5 at higher temperatures the breakdown voltage is lower and hence, after being generated by the Zener mechanism, the carriers will have a lower average energy: this is certainly one of the reasons which causes the decreases of EL intensity by increasing temperature (see Fig. 4).

3. Efficiency and limitations

We have also measured the EL intensity under reverse bias at different temperatures (in the range 77 to 473 K) as a function of current density in a large interval (0–150 A/cm^2). The data are summarized in Fig. 6. At each temperature the EL yield first increases linearly with fluence and eventually saturates. The rate at which the EL increases before saturation decreases when the temperature is increased but eventually the same saturation value is approached independently of temperature. These results indicate that at a sufficiently high current density (~ 100 A/cm^2 at 300 K) all the excitable Er sites have been excited and hence population inversion of all the excitable Er ions has been achieved. The saturation is not the result of a change in the fraction of hot carriers at higher current densities. In fact, in Fig. 7, we show that in the same current density region no saturation is observed in the signal arising from hot carriers (as measured at 1.2 μm). This signal in fact increases linearly with current density.

From the measurements reported in Fig. 6 some conclusions can be drawn on the quantum efficiency of these devices. The electroluminescence yield (EL) is proportional to the number of excited Er ions at steady state (N^*_{Er}), i.e.

$$EL \propto N^*_{Er}/\tau_{rad}, \quad (1)$$

where τ_{rad} is the radiative lifetime of the excited Er ions. The number of excited Er ions can be derived from the rate equation considering excitation through

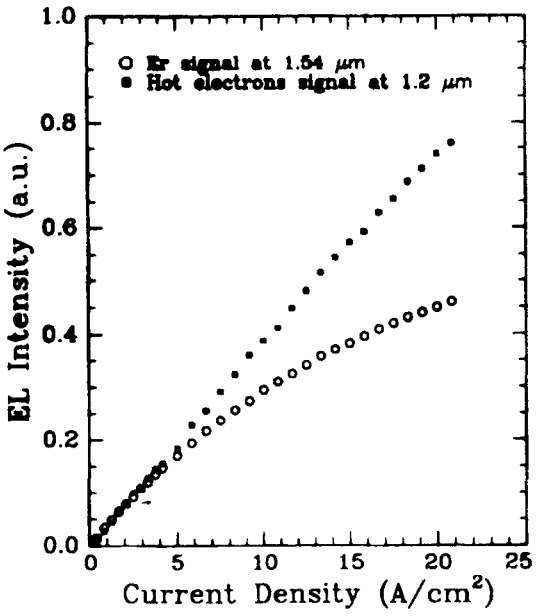

Fig. 7. Electroluminescence yield as a function of current density measured at 1.54 μm (Er signal) and at 1.2 μm (hot electron signal). This last curve has been multiplied by a factor of 4 for comparison.

impact ionization and deexcitation through both radiative and nonradiative channels:

$$\frac{dN_{Er}^*}{dt} = \sigma\phi(N_{Er} - N_{Er}^*) - \frac{N_{Er}^*}{\tau} \quad (2)$$

where σ is the cross section for impact excitation, ϕ the flux of hot electrons passing through the junction, N_{Er} the concentration of excitable Er ions and τ is the total deexcitation lifetime. At steady state the number of excited Er ions, N_{Er}^* is given by:

$$N_{Er}^* = \frac{\sigma\tau\phi}{\sigma\tau\phi + 1} N_{Er}. \quad (3)$$

At high pump power (when $\sigma\tau\phi >> 1$) all the Er ions are excited, i.e. $N_{Er}^* = N_{Er}$. In these conditions the EL intensity saturates at its maximum value EL_{sat}. Therefore:

$$\frac{EL}{EL_{sat}} = \frac{\sigma\tau\phi}{\sigma\tau\phi + 1}, \quad (4)$$

From the fit of the experimental data of Fig. 6 to Eq. (4) the value of $\sigma\tau$ at each temperature can be obtained. A value of 1.2×10^{-20} cm^2 s is obtained at RT, assuming that ~ 40% of the electrons passing through the junction are hot enough to excite erbium. Time-resolved electroluminescence measurements have shown that the decay time τ of the luminescence is ~ 30 μs. Hence we derive $\sigma = 4 \times 10^{-16}$ cm^2 for the impact excitation of Er. By using a calibrated power meter we were also able to measure a maximum emitted power of 10 μW and to calculate an internal quantum efficiency of 6×10^{-5} at 300 K. The maximum emitted power for a silicon LED is given by

$$P_{max} = \frac{hc}{\lambda} \frac{N_{Er}}{\tau_{rad}} \times AW, \quad (5)$$

where AW is the excitable volume (area times the depletion layer width). As $hc/\lambda = 0.8$ eV, $A = 0.05$ cm^2, assuming $\tau_{rad} = 1$ ms, and using the measured value of P_{max} we obtained:

$$N_{Er} \times W = 2 \times 10^{12}/\text{cm}^2,$$

which gives the total number of excitable Er ions in the depletion region. On the other hand the total number of Er atoms in the depletion layer is $\sim 4 \times 10^{13}$ /cm^2. This implies that only 5% of the incorporated Er ions are excitable even by impact excitation. This is clearly a major limitation which severely reduces the maximum emitted power and the internal quantum efficiency. A question arises on why most of the Er ions are not excitable. It should be noted that this number was deduced from the number of emitted photons at 1.54 μm. This number is proportional, according to Eq. (1), to the number of Er ions excited at steady state. Therefore, only those Er ions that can be efficiently pumped are counted. The large "inactive" fraction can therefore be due either to Er ions which are not in the 3+ state or to Er ions associated with fast nonradiative decay channels. These ions can still be excited but, since they decay very rapidly and nonradiatively, their contribution to the EL yield is negligible. Future work should certainly concentrate on methods to improve this fraction: for example the ratio of Er and O in the diode will probably need to be optimized since it determines the achievement of "ideal" Er sites which are 3+, can be pumped efficiently and are characterized by a reduced efficiency of the nonradiative channels.

4. Conclusions

Erbium incorporation in crystalline Si, with the aid of O codoping, has been shown to be a suitable method to obtain room temperature photo and electroluminescence at 1.54 μm. The mechanisms underlying Er excitation and the crucial steps towards the achievement of higher efficiency have been elucidated. It has been found that both Er photoluminescence and electroluminescence in Si diodes under forward bias are excited through electron–hole recombination. Optimization of the efficiency of this excitation mecha-

nism requires a proper engineering of the properties of the Er-related levels in the band gap which are the gateway for the energy transfer. This can be achieved by O codoping since the Er–O interaction results in the introduction of an Er-related level at $E_c - 0.15$ eV, through which efficient Er excitation can be achieved. Moreover, by suppressing the alternative routes for electron–hole recombination, O codoping also reduces the temperature quenching of the luminescence yield. The most efficient room temperature electroluminescence is achieved in an Er-doped Si diode under reverse bias. In this case Er pumping is shown to occur by hot carrier impact excitation of the Er ions with a cross section of 4×10^{-16} cm^{-2}. A maximum emitted power of 10 μW and an internal quantum efficiency of 6×10^{-5} have been achieved at room temperature. The major limiting factor for the efficiency of the diode has been identified as the small fraction of excitable Er ions which represents only $\sim 5\%$ of the total Er concentration.

References

[1] A. Taguchi, H. Nakagama and K. Takahei, J. Appl. Phys. 70 (1991) 5604.
[2] H. Ennen, J. Schneider, G. Pomrenke and A. Axmann, Appl. Phys. Lett. 43 (1983) 943.
[3] H. Ennen, G. Pomrenke, A. Axmann, W. Hayde and J. Scheneider, Appl. Phys. Lett. 46 (1985) 381.
[4] H. Issiki, K. Kobayashi, S. Yugo, T. Kimura and T. Ikoma, Appl. Phys. Lett. 58 (1991) 484.
[5] S.J. Chang and K. Takahei, Appl. Phys. Lett. 65 (1994) 433.
[6] J. Michel, J.L. Benton, R.F. Ferrante, D.C. Jacobson, D.J. Eaglesham, E.A. Fitzgerald, Y.H. Xie, J.M. Poate and L.C. Kimerling, J. Appl. Phys. 70 (1991) 2762.
[7] S. Coffa, F. Priolo, G. Franzó, V. Bellani, A. Carnera and C. Spinella, Phys. Rev. B 48 (1993) 11782.
[8] A. Polman, J.S. Custer, E. Snoeks and G.N. Van den Hoven, Nucl. Instr. and Meth. B 80/81, (1993) 653.
[9] S. Coffa, G. Franzó, F. Priolo, A. Polman and R. Serna, Phys. Rev. B 49 (1994) 16313.
[10] J.L. Benton, J. Michel, L.C. Kimerling, D.C. Jacobson, Y.H. Xie, D.J. Eaglesham, E.A. Fitzgerald and J.M. Poate, J. Appl. Phys. 70 (1991) 2667.
[11] G. Franzó, F. Priolo, S. Coffa, A. Polman and A. Carnera, Appl. Phys. Lett. 64 (1994) 2235.
[12] B. Zheng, J. Michel, F.Y.G. Ren, L.C. Kimerling, D.C. Jacobson and J.M. Poate, Appl. Phys. Lett. 64 (1994) 2842.
[13] G. Franzó, F. Priolo, S. Coffa, A. Polman and A. Carnera, Nucl. Instr. and Meth. B 96 (1995) 374.
[14] D.L. Adler, D.C. Jacobson, D.J. Eaglesham, M.A. Marcus, J.L. Benton, J.M. Poate and P.H. Citrin, Appl. Phys. Lett. 61 (1992) 2181.
[15] P.N. Favennec, H. l'Haridon, D. Moutonnet, M. Salvi and M. Gauneau, Jpn. J. Appl. Phys. 29 (1990) L524.
[16] I.N. Yassievich and L.C. Kimerling, Semicon. Sci. Technol. 8 (1993) 718.
[17] M. Needels, M. Schluter and M. Lannoo, Phys. Rev. B 47 (1993) 15533.
[18] F. Priolo, G. Franzó, S. Coffa, A. Polman, S. Libertino, R. Barklie and D. Carey, J. Appl. Phys. 78 (1995) 3874.
[19] S. Libertino, S. Coffa, G. Franzó and F. Priolo, J. Appl. Phys. 78 (1995) 3867.
[20] A.G. Chynoweth and M.G. McKay; Phys. Rev. 106 (1957) 418.
[21] W. Haecker, Phys. Status. Solidi. A 25 (1974) 301.
[22] M.R. Pinto, C.S. Rafferty and R.W. Dutton, *PISCES2–Poisson and Continuity Equation Solver*, Stanford Electronics Laboratory Technical Report, Stanford University (1984).
[23] G.A. Baraff, Phys. Rev. 133 (1964) A 26.